RNA (2001), *7*:435–444. Cambridge University Press. Printed in the USA.

Fending off decay: A combinatorial approach in intact cells for identifying mRNA stability elements

ZOFIA M.A. CHRZANOWSKA-LIGHTOWLERS and ROBERT N. LIGHTOWLERS

Department of Neurology, University of Newcastle upon Tyne, The Medical School, Framlington Place, Newcastle upon Tyne, NE2 4HH, United Kingdom

ABSTRACT

The strategy of systematic evolution, whereby nucleic acid sequences or conformers can be selected and amplified from a randomized population, has been exploited by many research groups for numerous purposes. It is, however, a technique largely performed in vitro, under nonphysiological conditions. We have now modified this in vitro approach to accomplish selection in growing cells. Here, we report that this new methodology has been used in vivo to select RNA elements that confer increased transcript stability. A randomized cassette was embedded in a 3′-untranslated region (UTR), downstream from the *luciferase* reporter open reading frame. A heterogeneous population of capped *luciferase* mRNA was then generated by in vitro transcription. Human liver Hep G2 cells were electroporated with this population of *luciferase* mRNA and total cytoplasmic RNA was isolated after varying lengths of incubation. Following RT-PCR, the 3′ UTR was used to reconstruct a new population of *luciferase* templates, permitting subsequent cycles of in vitro transcription, electroporation, RNA isolation, and RT-PCR. Increasing the incubation time at each cycle before RNA isolation imposed selection for stable transcripts. The functional half-life of the *luciferase* mRNA population increased from 55 to 140 min after four cycles. Subsequent sequencing of the selected 3′ UTRs revealed G-U rich elements in clones with extended chemical and functional half-lives.

Keywords: GU-rich elements; mRNA stability; posttranscriptional regulation; selection

INTRODUCTION

Messenger RNA is a key molecule in cell biology and the control of transcription plays a critical role in gene expression. It is not, however, simply the rate of production but the rate of mRNA decay that controls gene expression within cells. In most instances, mRNA stability and expression are effected by interplay of *cis*-acting elements in the nucleic acid with RNA-binding proteins acting in *trans*. Control of these RNA–protein interactions is not just fundamentally important to our understanding of cell biology, but is important in the pathogenesis of disease. Changes in mRNA stability, for example, have been implicated in the etiology of several neurological disorders (Amara et al., 1999; Canete-Soler et al., 1999), rheumatoid arthritis (Jeddi et al., 1994), and systemic scleroderma (Eckes et al., 1996).

Differences in stability can vary over several orders of magnitude, with half-lives ranging from several minutes for human lymphokine and cytokine mRNAs (Ross, 1995), to many hours for transcripts encoding members of the globin family (Weiss & Liebhaber, 1995) or respiratory chain components (Chrzanowska-Lightowlers et al., 1994). Stabilities of numerous mRNA species are known to be regulated in response to many forms of external stimuli, during development or at certain stages of the cell cycle. In most instances, it is the 3′ UTR that harbors the *cis*-acting sequences that are important in stability (Chkheidze et al., 1999; Jacobs Anderson & Parker, 2000; Mitchell & Tollervey, 2000), although examples outside this region have been identified (Canete-Soler et al., 1998).

Since the observation that an AU-rich element introduced into the 3′ UTR of transcripts could mediate selective mRNA degradation (Shaw & Kamen, 1986), research has focused on characterizing this element

Reprint requests to: Dr. Z.M.A. Chrzanowska-Lightowlers, Department of Neurology, University of Newcastle upon Tyne, The Medical School, Framlington Place, Newcastle upon Tyne, NE2 4HH, United Kingdom; e-mail: Z.Chrzanowska-Lightowlers@ncl.ac.uk.

(Chen & Shyu, 1995; Rajagopalan & Malter, 1996; Di Noia et al., 2000), the *trans*-acting proteins (Sela-Brown et al., 2000), and their importance in regulating mRNA decay. Although the factors defining rapid degradation began to be identified a decade ago (Shaw & Kamen, 1986), less has been achieved in identifying determinants that increase transcript stability. Polypyrimidine elements have been found in the 3′ UTRs of several long-lived mRNA species (Czyzyk-Krzeska & Beresh, 1996). Additionally, a family of poly-C binding proteins with homology to the hnRNP K polypeptides were shown to bind to the 3′ UTR stability element in β-globin mRNA (Chkheidze et al., 1999). Originally found in erythroid cells, this family of poly-C binding proteins is now known to be widely expressed and is believed to be associated with complexes that interact with the polypyrimidine tracts of other highly stable mRNA species (Holcik & Liebhaber, 1997).

The methodology described here was designed to identify any sequences or structures within a 3′ UTR that could confer increased mRNA stability. We demonstrate that this technique has been used successfully to select mRNA stability elements. This technology has enormous potential in the field of posttranscriptional regulation. As demonstrated here, it can be used for identifying RNA elements in both the 3′ and 5′ UTRs responsible not only for stabilizing transcripts in response to various extracellular stimuli, but also for localizing mRNA to subcellular compartments (Bashirullah et al., 1998; Tiedge et al., 1999). Moreover, having identified the *cis*-acting elements, any *trans*-acting factors can subsequently be detected and characterized by a variety of techniques.

RESULTS

To determine the power of our strategy for selecting RNA stability elements, two *luciferase* reporter templates containing randomized nucleic acid cassettes were constructed. The first was made with only a short, fully randomized 30mer 3′ UTR upstream from a poly(A)$_{30}$ tail and was constructed to act as a negative control for the selection process. The rationale was that because poly(A) binding proteins are known to interact with protein factors at the 5′ terminus (Imataka et al., 1998), it is possible that with only a short 3′ UTR, steric hindrance would prevent any potentially stabilizing complexes from forming. Consequently, no element should be capable of increasing transcript stability, precluding any selection for transcripts derived from template 1. The second template contained a larger, randomized 50mer embedded in a 3′ UTR from the human *COX4* mRNA (Fig. 1A). This particular UTR was chosen, as the ligation of full-length *COX* 3′ UTR downstream of the *luciferase* open reading frame (ORF) does not affect the stability of *luciferase* mRNA after transfection into Hep G2 cells (data not shown). This larger and more natural 3′ UTR was intended to provide the environment for selection of stability elements from the randomized cassette. A randomized N_{50} library theoretically provides 1.3×10^{30} unique 50mer permutations. It is therefore impossible to electroporate a sufficient quantity of RNA to cover all combinations. Indeed, we estimate that for the initial cycle, a maximum of 3×10^{11} unique combinations of 3′ UTRs could be imported by electroporation (Z. Chrzanowska-Lightowlers and R. Lightowlers, unpubl. observation). It is difficult to predict the minimum length requirement for a stability element. However, instability elements have been shown to function efficiently with only a nonamer sequence (Zubiaga et al., 1995). Only 2×10^5 permutations would be the minimum to cover every possible nonamer. Consequently, an N_{50} in template 2 was chosen as a compromise.

Transcripts selected from template 1 fail to show any increased stability

Template 1 was constructed as detailed in Materials and Methods. By positioning the randomized cassette downstream of the *luciferase* ORF, the functional half-life of the mRNA population can be calculated from the luciferase activity. Cell lysates were assayed for luciferase activity at various time intervals postelectroporation. Assuming the selected RNA element does not affect translational efficiency, the functional half-life of *luciferase* mRNA is defined as the time required to reach 50% of the maximum accumulation of luciferase activity (Gallie, 1991). A heterogeneous population of capped *luciferase* mRNA was transcribed from this template, electroporated into HeLa or Hep G2 cells and subjected to cycle selection as shown diagrammatically in Figure 1B. Cytoplasmic RNA was isolated at 5, 7, 10, 19, 22, and 24 h postelectroporation for HeLa and 10, 18, 24, and 28 h for Hep G2 cells, respectively. The functional half-life of the fully randomized *luciferase* mRNA population was calculated as 113 min in HeLa and 53 min in Hep G2 cells. To maximize the potential of selecting for stabilized transcripts, cytosolic RNA was isolated at increasing time points for each cycle postelectroporation, with the electroporated RNA being left for 24 or 28 h in the final cycle. No change in the profile of luciferase activity was observed even after the sixth cycle in HeLa or fourth cycle in Hep G2 cells (Fig. 2A,B). To compare the functional half-life with the chemical stability of the mRNA, RNase protection assays were performed on aliquots of RNA isolated from cells at the beginning and end of the cycle selection. The RNase assays confirmed that there was essentially no change in chemical mRNA half-life (chemical half-life of the selected population was 1.1-fold more stable—data not shown).

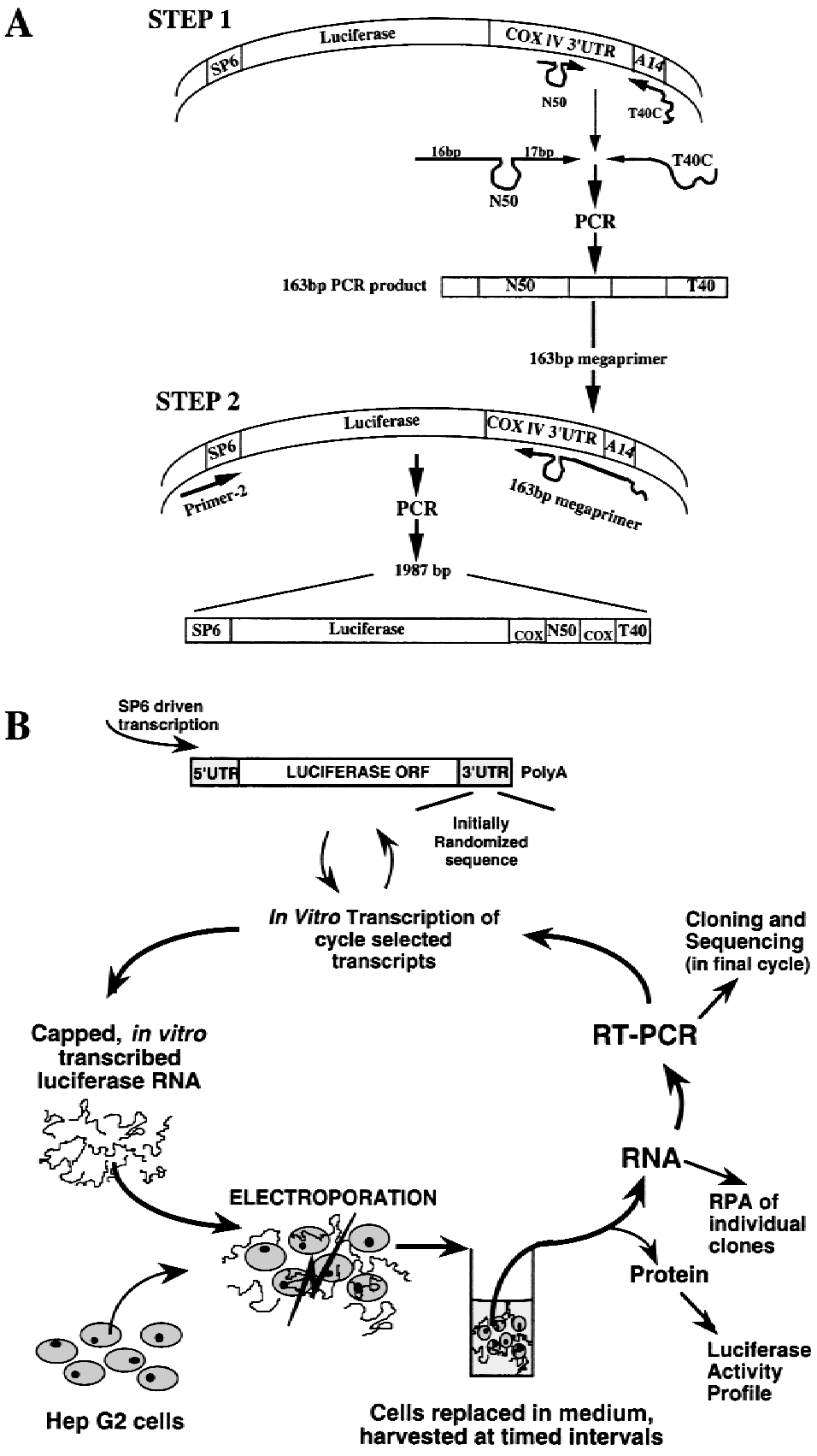

FIGURE 1. Construction of template 2 and schematic of in vivo cycle selection methodology. **A:** To determine the efficacy of the cycle selection, it was necessary to embed a randomized element into the 3′ UTR of a reporter mRNA. First, a natural untranslated region was provided by ligating the *COX4* 3′ UTR downstream from the *luciferase* ORF. A fully randomized N_{50} was then inserted in a two-step process detailed in Materials and Methods. **B**: Capped transcripts generated in vitro from either template 1 or 2 are electroporated into cultured cells. At various time points postelectroporation, an aliquot of cells is lysed and luciferase assays are performed. Selection for stabilized transcripts is imposed on each cycle by increasing the maximal incubation time postelectroporation before extraction of cytoplasmic RNA. Templates are reconstructed after subsequent RT-PCR by ligating the rescued 3′ UTR to new *luciferase* ORF to prevent the accumulation of PCR-generated mutations. Reconstructed templates are then subjected to in vitro transcription, completing the cycle. After the final cycle, products from the RT-PCR are cloned and sequenced to identify stability elements.

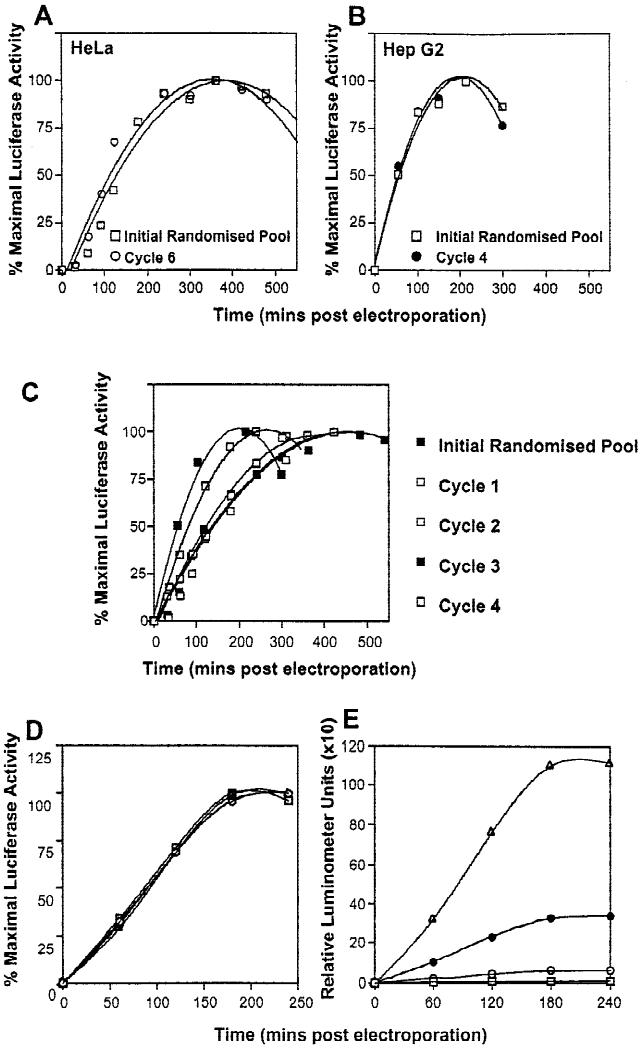

FIGURE 2. Template 2-generated transcripts are selected with increased stability. Cycle selection was performed with template 1- or template 2-derived transcripts electroporated into HeLa or Hep G2 cells. Aliquots of cells were isolated during each of the cycles at the indicated times, postelectroporation. Luciferase assays were performed and the functional half-life of the electroporated RNA calculated from the plot of maximal luciferase activity against time (Gallie, 1991). Four or six cycles of selection with template 1-derived RNA failed to influence the luciferase profile in either HeLa cells (**A**) or Hep G2 cells (**B**) respectively, indicating that no change in *luciferase* mRNA stability had been achieved. Conversely, a marked increase in the functional half-life of mRNA transcribed from template 2 was noted after each of the first three selection cycles, following electroporation into Hep G2 cells (**C**). The transfection and translation process is not saturated, as illustrated in **E**, as differences in relative luminometry units are still increased by using more RNA for the electroporation and by treating cells with DMSO. The plot of maximal luciferase activity against time is unaffected (**D**). Symbols in **D** and **E** represent the following amounts of mRNA electroporated: □: 0.2 μg, ○: 2 μg, ●: 2 μg + DMSO, △: 8 μg + DMSO.

Transcripts from template 2 show an increase in functional half-life following cycle selection

Template 2 was transcribed and the resultant population of *luciferase* mRNA was subjected to a similar selection cycle. Luciferase activity profiles are shown for cells electroporated with *luciferase* mRNA for each of four cycles, with cytoplasmic RNA isolated at 7, 11, 22, and 28 h postelectroporation. As shown in Figure 2C, the functional half-life for the mRNA population increased after each cycle of selection, ranging from 55 min for the fully randomized, to 140 min after cycle 4. The experiment was terminated after four cycles, as there was only a minimal increase in stability noted after this cycle. Based upon the efficiency of translation of the in vitro-transcribed RNA in reticulocyte lysate, together with ethidium bromide staining in formaldehyde gels, it was considered that equal amounts of *luciferase* mRNA were being used in each cycle to electroporate cells (40 μg initially and 5–8 μg RNA for the selection cycles). Nevertheless, to determine whether this progressive stability could have been due to differences in transfection efficiencies and saturation of translation or degradation mechanisms, luciferase activity profiles were compared after electroporation of cells with various amounts of RNA rescued from cycle 1. Figure 2E shows luciferase activity plotted as relative luminometer units against time postelectroporation for different amounts of RNA per electroporation and Figure 2D as a percentage of maximal activity against time postelectroporation. In addition, recent reports have indicated an increased efficiency of DNA transfection when performed in the presence of DMSO with a further increase if the cells are incubated in medium supplemented with DMSO postelectroporation (Melkonyan et al., 1996). As shown in Figure 2E, increasing amounts of electroporated RNA gave proportionally increasing luciferase activity in cell lysates, with an approximately fourfold improvement in electroporation efficiency in the presence of DMSO, confirming that DMSO treatment also increased transfection efficiencies of RNA. Second, the slope of the curves depicted in Figure 2E reflects the translation rate (Tanguay & Gallie, 1996) and although these varied as a consequence of RNA amounts used per electroporation, the point at which maximal protein accumulation was achieved remained the same. Thus, no change in translational profile was discernible when the activity was represented as a percentage of maximal luciferase activity (Fig. 2D). The differences observed in functional half-lives for the population of *luciferase* mRNA was therefore unlikely to be due to any differences in amounts or efficiencies of RNA electroporated into cells.

Luciferase mRNA reconstituted with cloned 3′ UTRs from cycle 4 show increased stability

Cycle selection generated a population of *luciferase* mRNA that had an increased functional half-life. If the increase was indeed due to RNA elements in the 3′ UTR cassette, it should be possible to isolate individual 3′ UTRs from the population that could impart an increased stability to a naïve RNA molecule. To test this

assumption, an aliquot of RNA isolated from cells 28 h after electroporation from cycle 4 was subjected to RT-PCR and the resultant product cloned into pGEM T-easy. Regions containing the randomized N_{50} were sequenced. Six of these sequences were chosen at random and ligated downstream of the *luciferase* ORF in pGEM-*luc*. Capped mRNA was synthesized in vitro and luciferase activity profiles from cells electroporated with either the clonal mRNAs or the original unselected RNA population were generated (Fig. 3A). All clones showed marked increases in functional half-lives when compared to the initial population of unselected RNA (55 min), ranging from 94 min (clone 166) to 225 min (clone 84). For four of these clones the functional half-life exceeded that achieved for the population in the final round; these were subjected to further analysis.

Selected mRNAs from template 2 are more stable

To confirm that the change in luciferase activity profile was truly a consequence of increased transcript stability, chemical half-life of these *luciferase* mRNA clones was measured directly. Messenger RNA from each clone was generated and electroporated into cells. RNA was extracted at various time points postelectroporation, and subjected to northern analysis using a random primed DNA fragment corresponding to the *luciferase* ORF.

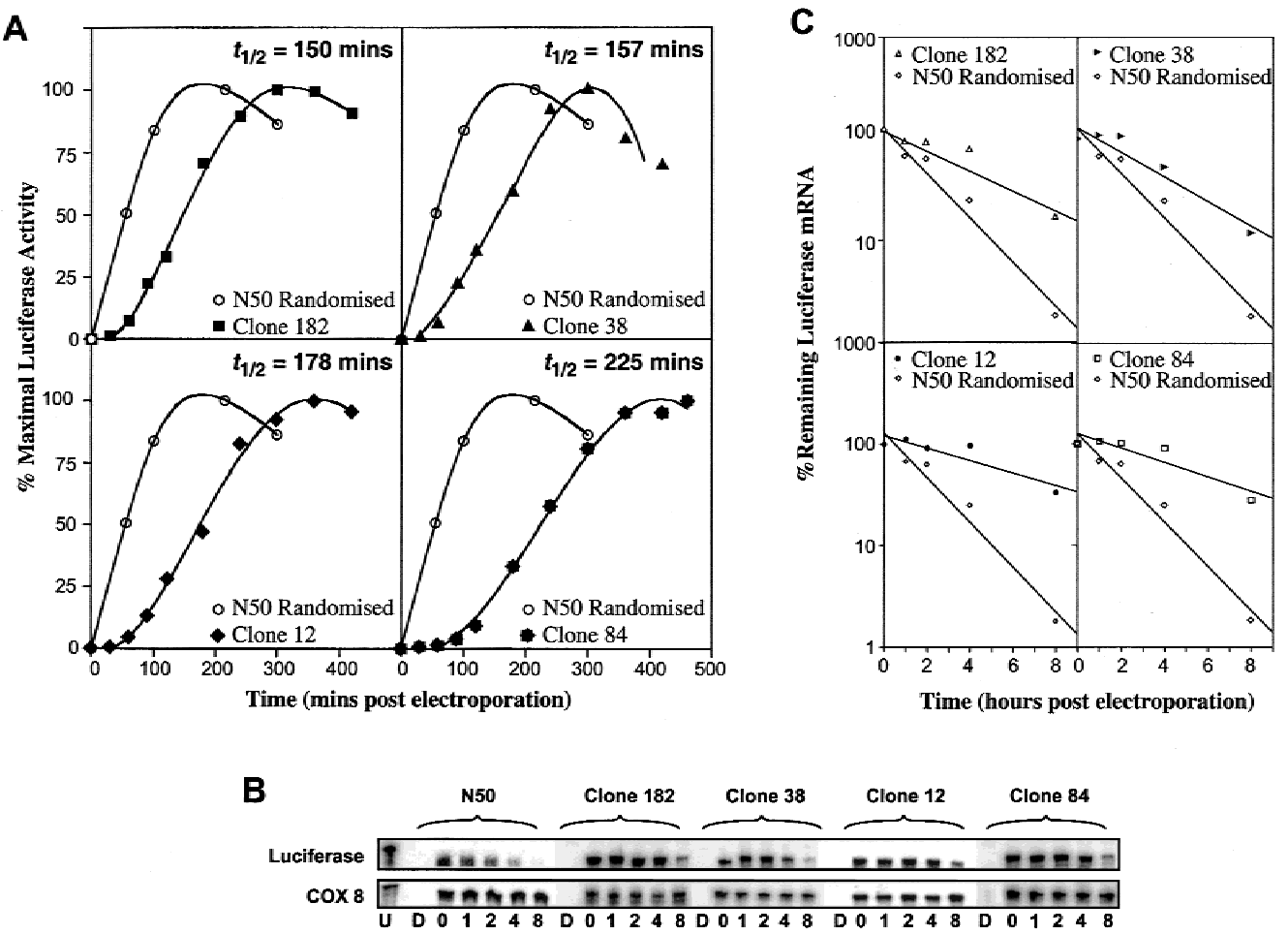

FIGURE 3. Individual clones selected from template 2-derived transcripts show increased stability. Selected sequences were rescued from cycle 4 by RT-PCR and recloned downstream from a *luciferase* ORF. **A**: Following transcription and electroporation into Hep G2 cells, luciferase activity was monitored and a luciferase profile constructed for each clone. The functional half-life, determined by the half-maximal activity, shows different values for each of the clones, all of which are in excess of the original randomized population. A representative of three independent profiles is given for each clone. **B**: To confirm that the increase in functional half-life reflected an increase in mRNA chemical stability when measured directly, RNase protection was performed. Transcripts from clones or original unselected template 2 were electroporated and cytoplasmic RNA extracted at times postelectroporation (0 to 8 h). RNase protection was performed with antisense probes for *luciferase* and *COX8*. Since both probes contained short ~50 nt 5′ vector sequence, it was possible to distinguish the undigested (U) from bound and protected probe. Probe subjected to digestion in the absence of cellular RNA is shown (**D**). **C**: To directly calculate the stability of these transcripts, semilog plots were derived from quantification of RPA results for both unselected (N_{50}) and clone RNA after correction for loading using the *COX8* control.

This proved to be unreliable at detecting the low levels of both *luciferase* and control transcript and so RNase protection (RPA) was used as a more sensitive alternative to detect and quantify the mRNA in the samples. Cytoplasmic RNA was isolated at various time points postelectroporation from cells electroporated either with transcripts derived from representative clones (clones 12, 38, 84, and 182) or from template 2 prior to selection. Figure 3B shows the RPA performed with an antisense fragment of *luciferase* RNA and the antisense RNA of a transcript encoding subunit VIII of cytochrome *c* oxidase (*COX8*) that acts as an internal control. Signals were quantified using ImageQuant software (Molecular Dynamics) and values for the *luciferase* signal corrected relative to the control. Graphing these values as a percentage of the remaining signal against time (semilog plot, Fig. 3C) allowed relative decay rates of the introduced *luciferase* transcript to be estimated. All four clones showed a greater stability than the randomized population, irrespective of the method used to measure half-life. There was a variation between the chemical and functional half-life, the former generally being greater than the latter. However, for each of the four clones, the relative hierarchy of increased stability was similar whether calculated by functional or chemical half-lives. This confirms that the method had successfully selected stable mRNAs from within the original population.

Analysis of selected sequences

Analysis for motifs was performed both by visual inspection and computer searches (MEME, UTRscan, PATscan) on the selected sequences from the 30 and 36 clones derived from the final round of selection from templates 1 and 2, respectively. Sequences from template 2 contained a higher than random distribution of G and U nucleotides and were A-poor (Table 1). This contrasted strongly with the clones derived from template 1, where no nucleotide bias was observed (available on request). Many -GG- and 16 G-quartets were identified in template 2 sequences, moreover clone 84, which demonstrated the longest half-life, contained three such 4G motifs. Interestingly, nucleotide sequences con-

TABLE 1.

A. Manual alignment of a subset of selected sequences

```
182                                                  GUUUUGG|CCGUACC(UUGUUGUGUGUGACC)GAC GGGUGUACUUGGUCCUCG
38                                       GGCU UGCGUUCGUUCAAGGUAGUGG|GUCAAUCGGC                GGGGAUGUGCCCCCU
84                                                 GGGGACGGAUUGG|UCCGACUAUCGU                AGGGGAGUCGACUGUUGAUCCGGGG
12          UCCCCUGCUUCUGGCUAAUAUUACUUGUAUCUGCGGUACUCAGUUUGG|CC
166 GAACAGGGUCGAACCCAGGUGUUUAACG CUGCGACCU  GCUGAAUUGUUGG|
166                 GAACAGG        GUC    GAACCC     AGGU GUUUAA|C GCUGCGACCUGCUGAAUUGUUGG
55                CUNUUUGG    GNCGGNGCCU  ACCCCCGGGGAGNGUUAGG|AGGGAAGUGUGGC
11          CGUCCGAGGCGUGGUUAAG    UCCU CGACC GACUCGGUGGUUUGG|AAUGAG
112           AAAUUGGCCUGG       UCUCCU  GAC        GGAGGUUUGG|GUGCUCCGAUUUGUGCG
G61     CACUGAGGGGU GUGGAUAGUAAGUCCUGUGUGCAC   CGG  GUUUGU|CGUUUUUA
G56   UCUCUGCCAAAUAGUUG      UGCUCCUCAGGGGCAG CUGGACGGUGUG|CAUGU
4           CGGGGUUGUGG    CAUUGUCCGAUCAUGUUUGUAGCAUGCUUGG|CAG
G45                                                  CUUUGG|GUGUCAUAGAUUGCGCAGGCC     UAGGCU GAACUUCCUUGCGCGG
55                                                 CUNUUUGG|GNCGGNGCCUACCCCCGGGGAGNGUUAGGAGGGAAGUGUGGC
55      CUNUUUGGGNCGGNGCCUACCCCCGGGGAGNGUUAGGAGGAAGUGUGG|C
G62                                              UCAGGUGGUUUCA|AGGCUCUGUCUAUGGUUAGCCC          GGGAGAGUCUUCCGAU
G86                                                CUCUGUUUGA|UUGGCUGUCGCGU GUUGCUAACUCAGAGAGGGGAGUGCAG
160               AUUUGC     GGGGUCCGGGGACCA      UUGUG UUGG|G UG
4           CGGGGUUGUGG    CAUUGUCC             GAUCAUGUUUGU|AGCAUGCUUGGCAG
```

B. MEME-derived consensus **UUUUGGCUGAACCGAGUUGUGU**

Clone	start position in N50		Matches/22
182	2	UUUUGGCCGUACCUUGUUGUGU	18
112	27	GUUUGGGUGCUCCGAUUUGUGC	16
12	9	UUCUGGCUAAUAUUACUUGUAU	14
G45	1	CUUUGGGUGUCAUAGAUUGCGC	10
G45	26	CCUAGGCUGAACUUCCUUGCGC	13
160	11	UCCGGGGACCAUUGUGUUGGGU	10
166	3	ACAGGGUCGAACCCAGGUGUUU	13
169	25	UGUGGGCUUACCGGAUUCGUUU	14
164	5	UUAUAGGCUAAUCGCGUCGUGA	12
G39	1	ACAUUGUCCAAUGGGUUUAUGU	10
G31	22	AGUGGUCAGUACCCAGUUGGUU	13
4	12	CAUUGUCCGAUCAUGUUUGUAG	11

taining -GGGG- or multiple -GG- motifs have been shown to generate extremely stable higher order intramolecular structures that may confer nuclease resistance (Kim et al., 1991; Cheong & Moore, 1992; Bishop et al., 1996). In the reported cases, however, the strong secondary structures generated in G-rich sequences only confer nuclease resistance when located at a 5′ or 3′ terminus (Muhlrad et al., 1995) and do not promote a dominant increase in stability to the entire RNA molecule (Decker & Parker, 1993).

Template 2 sequences were manually aligned for perceived patterns (Table 1A). The main focus was a GU-rich motif centered on CGGNGGUUUGG. When all the sequences were subjected to MEME analysis, the resultant consensus motif also included UUUGG (Table 1B). Previous work has shown that polypyrimidine stretches can play an important role in stabilizing certain mRNA species (Weiss & Liebhaber, 1995; Czyzyk-Krzeska & Beresh, 1996; Kohn et al., 1996; Chkheidze et al., 1999). Although polypyrimidine motifs were identified by PATscan and UTRscan these did not exceed four consecutive bases in any selected sequence. Additionally, one nanos translational control element motif was identified (clone G33; Dahanukar & Wharton, 1996). BLAST searches were performed on all template 2 selected sequences and the MEME-derived consensus; all gave at least one correspondence with the human genome and many in intergenic sequences from other species. One example is clone 182, which is highly GU-rich and has a tract of the N_{50} represented in the MEME-derived consensus. Moreover, it has a 15-nt stretch (in parentheses in Table 1A) which has 100% identity to part of the 3′ UTR of human *glutathione transferase zeta-1* mRNA (Fernandez-Canon & Penalva, 1998) and at least 15 intergenic regions from within the *Arabidopsis* database.

DISCUSSION

These results show that RNA elements embedded in the 3′ UTR can substantially affect the stability of an entire, mature mRNA. By using the combinatorial approach described here, such stability elements were successfully selected from a randomized pool. Selected sequence cassettes (template 2) containing stability elements are compared in Table 1. Although motifs can be determined both visually and using MEME, the redundancy of this consensus is surprising. One aspect however, is shared by all the stability elements—the high level of guanine and uridine bases and GU-rich elements. Within the MEME-derived consensus sequence, 16 of the 22 positions are G or U nucleotides. This is in contrast to other known stability elements that contain polypyrimidine tracts and are bound by a family of poly-C binding proteins (Holcik & Liebhaber, 1997; Czyzyk-Krzeska & Bendixen, 1999). Such previous data predict that at least a subset of selected elements should have been rich in polypyrimidines, but this was not found. In our study, complete sequence concordance was not observed and different clonal mRNAs would be expected to exhibit different half-lives. This was indeed the case, with each of the clones assayed exhibiting increased stability over the initial randomized population. In fact, the disparity between sequences together with their increased but differing functional and chemical half-lives makes it highly unlikely that selected stability elements derived their increased stability by a common interaction with the body of the *luciferase* mRNA molecule or a secondary structure intrinsic to the *luciferase* reporter. It is therefore likely that these elements can act independently to promote stability of most transcripts, an area that is currently being pursued.

As predicted, stability elements were not selected in mRNA transcribed from template 1. Although not shown directly, it is possible that the lack of selection from template 1 was due to steric constraints preventing the binding of *trans*-acting proteins. Furthermore, as template 1 encoded transcripts with a shorter poly(A) tail than those from template 2, these may have been more susceptible to rapid, deadenylation-dependent decay (Beelman & Parker, 1995).

Initially designed to identify generic stability sequences, this in vivo technology also has substantial potential for identifying *cis*-acting RNA elements that promote stability of transcripts in response to many different types of stimuli. Metabolic acidosis, for example, is associated with numerous diseases, and recent research has unveiled a pH-responsive element in the 3′ UTR of rat renal glutaminase mRNA (Hansen et al., 1996) that, together with a specific *trans*-acting protein, effects changes in transcript stability (Laterza et al., 1997). Similarly, hypoxic culture conditions can mimic clinical ischemia with recognized changes in stability of a number of transcripts (Semenza et al., 1994; Maity & Solomon, 2000). Finally, another area of research that is likely to benefit from this in vivo selection methodology is mRNA localization. Identification of elements that localize RNA species to the nucleus has been achieved using another method also based on selection from a combinatorial library (Grimm et al., 1997). Grimm and colleagues used this method to select *cis*-acting elements that promote nuclear localization of RNA. The RNA species used in the study were synthesized to resemble small nuclear RNAs carrying a strong nuclear export signal in the form of a m^7G cap. A combinatorial library was inserted into this RNA moiety. Species were selected on their ability to override the strong export signal and become localized or be retained in the nucleus following cytoplasmic or nuclear injection, respectively. In addition to the nuclear RNA species that are the focus of the above mentioned study, many messenger RNA species are now known to be localized to subcellular compartments, although the

physiological relevance of this process is largely obscure (Chang et al., 1997; Kislauskis et al., 1997; Tiedge et al., 1999). Use of the selection cycle presented here coupled with relevant subcellular fractionation will allow *cis*-acting elements to be identified that function to localize mRNA species to subcellular locations within cells. We believe that this technique provides a valuable tool with great potential for investigating and dissecting the mechanisms involved in posttranscriptional regulation.

MATERIALS AND METHODS

Tissue culture

All tissue culture media and supplements were purchased from Sigma and all plasticware from Corning-Costar. HeLa and human liver Hep G2 cells were cultured in Eagle's modified essential medium supplemented with 10% fetal calf serum, nonessential acids and 2 mM L-glutamine.

Template production

Template 1

Primer 1.1 (5′-$T_{30}N_{30}$TTACAATTTGGACTTTCCGCC-3′) incorporates sequence to generate a poly(A) tail and a randomized 3′ UTR of 30 nt as well as sequence corresponding to the 3′ end of the *luciferase* ORF. It was used in conjunction with Primer 1.2 (5′-CAAGCTATTTAGGTGACACTATAGAA TACTCAAGCTTATGC-3′), which corresponds to the 5′ end of *luciferase* and includes an SP6 RNA polymerase recognition site. PCR reactions were performed in 100 μL with final concentrations of 1.5 mM $MgCl_2$, 1 $\times$ reaction buffer IV (ABgene, Surrey, UK), 200 μM dNTPs, 100 pmol of each primer, 10 ng pGEM-*luc* template (Promega) and 2 units thermostable DNA polymerase (ABgene, Surrey, UK). Hot start reactions were initiated by adding the enzyme after a 4 min denaturation step, followed by 30 cycles of 94 °C for 1.5 min, 59 °C for 1 min, 72 °C for 3 min, and a final 8 min extension. The resulting DNA product then contained all the elements required for SP6-driven in vitro transcription to produce a polyadenylated *luciferase* mRNA containing an N_{30} randomized 3′ UTR.

Template 2

To generate the second template, the 3′ UTR of the gene encoding human cytochrome *c* oxidase subunit IV (*COX4*) was first inserted downstream of the *luciferase* ORF. The 3′ UTR from human *COX4* gene was liberated from p*COX4.111* (Zeviani et al., 1987) by *Eco*RI then *Sfa*NI digestion and filled in using Klenow fragment. This 146-bp fragment (bases 537–682; Zeviani et al., 1987) was ligated into *Stu*I-digested pGEM-*luc*, and construct confirmed by sequencing.

Template 2 containing the N_{50} cassette was then synthesized by a two-step PCR procedure (Fig. 1A). In Step 1, Primer 2.1 (5′-T_{40}CAGGTAAACTGG-3′) was used with Primer 2.2 (5′-CCATGCAACTCCATGCCN$_{50}$CTGGAAACCTGTTA TGC-3′). The former provided an extended poly(A) tail at the 3′ terminus of the *COX*-UTR and the latter incorporated the N_{50} cassette while hybridizing at both its 3′ and 5′ ends to the *COX*-UTR. PCR reactions were as for template 1, but with the following profile: 30 cycles of 95 °C for 1 min, 45 °C for 30 s, 72 °C for 20 s, and a final 8 min extension. This 164-bp product contained the randomized cassette embedded in the 3′ UTR and a poly$(A)_{40}$ tail. After gel purification (Qiagen) this PCR product ($\sim$2 pmol) was used as a megaprimer in conjunction with Primer 1.2 in Step 2 (Fig. 1A). Following initial denaturation and enzyme addition, 30 cycles of 95 °C for 1.5 min, 59 °C for 1 min, and 72 °C for 3.5 min were performed with a final 8 min extension.

Methodology for cycle selection

Capped *luciferase* mRNA species were generated by high yield phage SP6-driven in vitro transcription in the presence of ^{m7}G(5′)ppp(5′)G cap analog following manufacturer's recommendations (all reagents from Epicentre, Cambio, UK). RNA was analyzed for integrity and concentration by denaturing gel electrophoresis and efficiency of translation in rabbit reticulocyte lysate (nuclease treated, Promega). Reactions were programmed with equal amounts of in vitro-transcribed, capped RNA and performed as per manufacturer's instructions. Translation of *luciferase* was assessed by luminometry (Turner Instruments TD-20e); Luciferin substrate (35 μL) and reticulocyte lysate (2 μL) were combined and light emission measured immediately for 3 $\times$ 10 s periods.

To initiate each cycle, in vitro-transcribed, capped mRNA (20 μg cycle 1, between 5–8 μg for subsequent cycles) was combined with 9 $\times$ 10^6 Hep G2 cells in 0.5 mL ice cold PBS (with or without DMSO, 1.25% [v/v]) and electroporated immediately in 0.2-cm path-length cuvettes. BioRad Genepulser II parameters were 400 V and 250 μF. Cells were transferred to prewarmed culture medium (with or without DMSO) at a density of 1 $\times$ 10^6 cells per mL and incubated at 37 °C.

Aliquots of 0.5 $\times$ 10^6 cells were harvested at intervals postelectroporation, lysed in 40 μL cell lysis buffer (Promega) and luciferase activity measured as above using 15 μL lysate and 40 μL substrate. Assays were performed in triplicate and average values used to plot luciferase activity as a percentage of maximal activity. These profiles were used to calculate the functional half-lives of the transcripts. RNA was extracted from 4 $\times$ 10^6 cells using Trizol (Gibco-BRL, manufacturer's instructions). RT-PCR (Superscript Pre-amplification system, Gibco-BRL) was effected following manufacturer's recommendations as a two-step procedure. Ten micrograms of cytosolic RNA served as template for reverse transcription with 50 pmol of reverse primer, Primer T_{30}, or Primer 2.1. PCR was performed using Primer T_{30} or 2.1 with Primer 3 (5′-CGAATTATGTGTCAGAGGACC-3′), which is internal to the *luciferase* ORF and spans the *Cla*I restriction site. After *Cla*I digestion, the product containing the 3′ UTR was gel purified. Repeated PCR of the *luciferase* ORF would have generated DNA polymerase induced errors, so pGEM-*luc* was *Cla*I/*Nde*I digested to give a scaffold to which the RT-PCR selected 3′ UTR sequences were ligated. These products were ligated overnight to produce an intact *luciferase* DNA template containing the selected 3′ UTR sequences. Subsequent PCR regenerated full-length *luciferase* template using Primer T_{30} or 2.1 in tandem with Primer 1.2 (profile as for template 1

production) providing template for the next cycle of in vitro transcription.

Sequencing and reconstruction of individual luciferase templates

PCR products were generated from the final selection cycle using Primer T_{30} or 1a with Primer 4, internal to the 3′ coding region of *luciferase* (5′-GAGCACGGAAAGACGATG-3′). These products were then ligated into pGEM T-easy (Promega) to facilitate sequencing. DNA was cycle sequenced using Big Dye terminator cycle sequencing ready reaction kits (PE Biosystems) and samples electrophoresed on an ABI 377 sequencer. A number of clones were then digested with *Eco*NI and *Sac*I to allow the selected sequence to be ligated downstream of the *luciferase* ORF (pGEM-*luc Eco*NI and *Sac*I digested).

Analysis of selected sequences

Cycle 4 sequences from both templates 1 and 2 were analyzed manually for motifs and nucleotide content. Individual sequences were compared with database entries using Advanced Blast (Altschul et al., 1997), PATscan (Jacobs et al., 2000), UTRscan (www.ba.cnr.it; Pesole & Liuni, 1999) and subjected to MEME motif searching (Bailey & Gribskov, 1998). Individual 3′ UTR sequences positioned downstream of *luciferase* as described above were subjected to in vitro transcription. These and control, randomized 3′ UTR mRNAs were separately electroporated into cells with subsequent preparation of nine protein lysates and five RNA extractions. Protein and RNA aliquots were then analyzed by luminometry (in triplicate as previously described) and RPA, respectively.

RNase protection assays

In vitro-transcribed, capped mRNA (30 μg) was electroporated into 17.5×10^6 Hep G2 liver cells as described above. For RNase protection assays (Ambion RPAIII) on the randomized population and individual clones, RNA was extracted from 3.5×10^6 cells per time point at 0, 1, 2, 4, and 8 h postelectroporation. Antisense probes were generated by radiolabeled, in vitro transcription (α-^{32}P UTP, 800 Ci/mmol, Amersham) to generate fragments of 315 nt of *luciferase* and 350 nt of p*COX8.21* (Rizzuto et al., 1989). Probes were purified from 5% denaturing polyacrylamide gels, eluted, and RPA performed with 60,000 cpm of probe and 10 μg extracted cytosolic RNA following manufacturer's recommendations. Digested samples together with probe controls were electrophoresed through 5% denaturing polyacrylamide gels and PhosphorImage analyzed (ImageQuant, Molecular Dynamics).

ACKNOWLEDGMENTS

Z.C.-L. and R.L. thank The Wellcome Trust for continued support and funding (Z.C.-L. is a Wellcome Trust Research Career Development Fellow). We thank Geoff Taylor for assistance with sequencing, the Canterbury Medical Research Foundation for awarding Z.C.-L. a Don Beaven Travelling Fellowship and Martin Kennedy (University of Otago, Christchuch School of Medicine, New Zealand) for encouragement and temporary laboratory space. We also thank Roy Parker for his incisive comments and suggestions.

Received July 13, 2000; returned for revision August 15, 2000; revised manuscript received December 4, 2000

REFERENCES

Altschul SF, Madden TL, Schäffer AA, Zhang J, Zhang Z, Miller W, Lipman DJ. 1997. Gapped BLAST and PSI-BLAST: A new generation of protein database search programs. *Nucleic Acids Res 25*:3389–3402.

Amara FM, Junaid A, Clough RR, Liang B. 1999. TGF-beta(1), regulation of Alzheimer amyloid precursor protein mRNA expression in a normal human astrocyte cell line: mRNA stabilization. *Brain Res 71*:42–49.

Bailey TL, Gribskov M. 1998. Methods and statistics for combining motif match scores. *J Comput Biol 5*:211–221.

Bashirullah A, Cooperstock RL, Lipshitz HD. 1998. RNA localization in development. *Annu Rev Biochem 67*:335–394.

Beelman CA, Parker R. 1995. Degradation of mRNA in eukaryotes. *Cell 81*:179–183.

Bishop JS, Guy-Caffey JK, Ojwang JO, Smith SR, Hogan ME, Cossum PA, Rando RF, Chaudhary N. 1996. Intramolecular G-quartet motifs confer nuclease resistance to a potent anti-HIV oligonucleotide. *J Biol Chem 271*:5698–5703.

Canete-Soler R, Schwartz M, Hua Y, Schlaepfer W. 1998. Stability determinants are localized to the 3′-untranslated region and 3′-coding region of the neurofilament light subunit mRNA using a tetracycline-inducible promoter. *J Biol Chem 273*:12650–12654.

Canete-Soler R, Silberg D, Gershon M, Schlaepfer W. 1999. Mutation in neurofilament transgene implicates RNA processing in the pathogenesis of neurodegenerative disease. *J Neurosci 19*:1273–1283.

Chang JW, Schumacher E, Coulter PM, Vinters HV, Watson JB. 1997. Dendritic translocation of RC3/neurogranin mRNA in normal ageing, Alzheimer disease and fronto-temporal dementia. *J Neuropath Exp Neurol 56*:1105–1118.

Chen C, Shyu AB. 1995. AU-rich elements: Characterization and importance in mRNA degradation. *Trends Biochem Sci 20*:465–470.

Cheong C, Moore PB. 1992. Solution structure of an unusually stable RNA tetraplex containing G- and U-quartet structures. *Biochem 31*:8406–8414.

Chkheidze AN, Lyakhov DL, Makeyev AV, Morales J, Kong J, Liebhaber SA. 1999. Assembly of the alpha globin mRNA stability complex reflects binary interaction between the pyrimidine-rich 3′ untranslated region determinant and poly(C) binding protein alpha-CP. *Mol Cell Biol 19*:4572–4581.

Chrzanowska-Lightowlers ZMA, Preiss T, Lightowlers RN. 1994. Inhibition of mitochondrial protein synthesis promotes increased stability of nuclear-encoded respiratory gene transcripts. *J Biol Chem 269*:27322–27328.

Czyzyk-Krzeska MF, Bendixen AC. 1999. Identification of the poly(C) binding protein in the complex associated with the 3′untranslated region of erythropoietin messenger RNA. *Blood 93*:2111–2120.

Czyzyk-Krzeska MF, Beresh JE. 1996. Characterization of the hypoxia-inducible protein binding site within the pyrimidine-rich tract in the 3′-untranslated region of the tyrosine hydroxylase mRNA. *J Biol Chem 271*:3293–3299.

Dahanukar A, Wharton RP. 1996. The Nanos gradient in *Drosophila* embryos is generated by translational regulation. *Genes & Dev 10*:2610–2620.

Decker CJ, Parker R. 1993. A turnover pathway for both stable and unstable mRNAs in yeast: Evidence for a requirement for deadenylation. *Genes & Dev 7*:1632–1643.

Di Noia J, D'Orso I, Sanchez D, Frasch A. 2000. AU-rich elements in the 3′-untranslated region of a new mucin-type gene family of *Trypanosoma cruzi* confers mRNA instability and modulates translation efficiency. *J Biol Chem 275*:10218–10227.

Eckes B, Mauch C, Huppe G, Krieg T. 1996. Differential regulation of transcription and transcript stability of pro-alpha1(I) collagen and fibronectin in activated fibroblasts derived from patients with systemic scleroderma. *Biochem J 315*:549–554.

Fernandez-Canon JM, Penalva MA. 1998. Characterization of a fungal maleylacetoacetate isomerase gene and identification of its human homologue. *J Biol Chem 273*:329–337.

Gallie D. 1991. The cap and poly(A) tail function synergistically to regulate mRNA translational efficiency. *Genes & Dev 5*:2108–2116.

Grimm C, Lund E, Dahlberg JE. 1997. In vivo selection of RNAs that localize in the nucleus. *EMBO J 16*:793–806.

Hansen WR, Barsic-Tress N, Taylor L, Curthoys NP. 1996. The 3′-nontranslated region of rat renal glutaminase mRNA contains a pH-responsive stability element. *Am J Physiol 271*:F126–131.

Holcik M, Liebhaber SA. 1997. Four highly stable eukaryotic mRNAs assemble 3′untranslated region RNA–protein complexes sharing *cis* and *trans* components. *Proc Natl Acad Sci USA 94*:2410–2414.

Imataka H, Gradi A, Sonenberg N. 1998. A newly identified N-terminal amino acid sequence of human eIF4G Binds poly(A)-binding protein and functions in poly(A) dependent translation. *EMBO J 17*:7480–7489.

Jacobs Anderson JS, Parker R. 2000. Computational identification of *cis*-acting elements affecting post-transcriptional control of gene expression in *Saccharomyces cerevisiae*. *Nucleic Acids Res 28*:1604–1617.

Jacobs GH, Stockwell PA, Schrieber MJ, Tate WP, Brown CM. 2000. Transterm: A database of messenger RNA components and signals. *Nucleic Acids Res 28*:293–295.

Jeddi PA, Lund T, Bodman KB, Sumar N, Lydyard PM, Pounce L, Heath LS, Kidd VJ, Delves PJ. 1994. Reduced galactosyltransferase mRNA levels are associated with galactosyl IgG found in arthritis-prone MRL-*lpr/lpr* strain mice. *Immunology 83*:484–488.

Kim J, Cheong C, Moore PB. 1991. Tetramerization of an RNA oligonucleotide containing a GGGG sequence. *Nature 351*:331–332.

Kislauskis EH, Zhu X-C, Singer RH. 1997. Beta-actin messenger RNA localization and protein synthesis augment cell motility. *J Cell Biol 136*:1263–1270.

Kohn DT, Tsai KC, Cansino VV, Neve RL, Perrone-Bizzozero NI. 1996. Role of highly conserved pyrimidine-rich sequences in the 3′ untranslated region of the GAP-43 mRNA in mRNA stability and RNA–protein interactions. *Brain Res 36*:240–250.

Laterza OF, Hansen WR, Taylor L, Curthoys NP. 1997. Identification of an mRNA-binding protein and the specific elements that may mediate the pH-responsive induction of renal glutaminase mRNA. *J Biol Chem 272*:22481–22488.

Maity A, Solomon D. 2000. Both increased stability and transcription contribute to the induction of the urokinase plasminogen activator receptor (uPAR) message by hypoxia. *Exp Cell Res 255*:250–257.

Melkonyan H, Sorg C, Klempt M. 1996. Electroporation efficiency in mammalian cells is increased by dimethyl sulfoxide. *Nucleic Acids Res 24*:4356–4357.

Mitchell P, Tollervey D. 2000. mRNA stability in eukaryotes. *Curr Op Genet Dev 10*:193–198.

Muhlrad D, Decker CJ, Parker R. 1995. Turnover mechanisms of the stable yeast *PGK1* mRNA. *Mol Cell Biol 15*:2145–2156.

Pesole G, Liuni S. 1999. Internet resources for the functional analysis of 5′ and 3′ untranslated regions of eukaryotic mRNAs. *Trends Genet 15*:378.

Rajagopalan L, Malter J. 1996. Turnover and translation of in vitro synthesized messenger RNAs in transfected, normal cells. *J Biol Chem* 271:19871–19876.

Rizzuto R, Nakase H, Darras B, Francke U, Fabrizi G-M, Mengel T, Walsh F, Kadenbach B, DiMauro S, Schon EA. 1989. The gene specifying subunit VIII of human cytochrome *c* oxidase is localized to chromosome 11 and is expressed in both muscle and non-muscle tissues. *J Biol Chem 264*:10595–10600.

Ross J. 1995. mRNA stability in mammalian cells. *Microbiol Rev 59*:423–450.

Sela-Brown A, Silver J, Brewer G, Naveh-Many T. 2000. Identification of AUF1 as a parathyroid hormone mRNA 3′-untranslated region-binding protein that determines parathyroid hormone mRNA stability. *J Biol Chem 275*:7424–7429.

Semenza GL, Roth PH, Fang H-M, Wang GL. 1994. Transcriptional regulation of genes encoding glycolytic enzymes by hypoxia-inducible factor-1. *J Biol Chem 269*:23757–23763.

Shaw G, Kamen R. 1986. A conserved AU sequence from the 3′ untranslated region of GM-CSF mRNA mediates selective mRNA degradation. *Cell 46*:659–667.

Tanguay R, Gallie D. 1996. Translational efficiency is regulated by the length of the 3′ untranslated region. *Mol Cell Biol 16*:146–156.

Tiedge H, Bloom FE, Richter D. 1999. RNA, whither goest thou? *Science 283*:186–187.

Weiss IM, Liebhaber SA. 1995. Erythroid cell-specific mRNA stability elements in the alpha-globin 3′ nontranslated region. *Mol Cell Biol 15*:2457–2465.

Zeviani M, Nakagawa M, Herbert J, Lomax MI, Grossman LI, Sherbany AA, Miranda AF, DiMauro S, Schon EA. 1987. Isolation of a cDNA clone encoding subunit IV of human cytochrome *c* oxidase. *Gene 55*:205–217.

Zubiaga AM, Belasco JG, Greenberg ME. 1995. The nonamer UUAUUUAUU is the key AU-rich sequence motif that mediates mRNA degradation. *Mol Cell Biol 15*:2219–2230.